Synthesis and Structure of BiCa$_2$VO$_6$

I. Radosavljevic, J. S. O. Evans, and A. W. Sleight[1]

Department of Chemistry and Center for Advanced Materials Research, Oregon State University, Corvallis, Oregon 97331-4003

A new compound, BiCa$_2$VO$_6$, has been synthesized and its structure determined. This compound crystallizes in space group *Cmc*2$_1$ (No. 36) with $a = 8.892$ Å, $b = 11.961$ Å, $c = 5.546$ Å, and $Z = 4$. Both high-resolution X-ray and neutron powder diffraction data were used in the refinement of the BiCa$_2$VO$_6$ structure. This structure can be described as composed of (BiO$_2$)$^-$ chains, VO$_4^{3-}$ tetrahedra, and Ca^{2+} cations leading to a BiO$_2$Ca$_2$VO$_4$ structural formula. This compound is potentially ferroelectric where switching polarity would mainly involve rotations of VO$_4$ tetrahedra. © 1998 Academic Press

INTRODUCTION

The bright yellow color of bismuth vanadate (BiVO$_4$) gives it considerable potential as a pigment, and this compound is also known to be ferroelastic (1). When BiVO$_4$ is suitably doped, it becomes a highly selective catalyst for the partial oxidation of propylene and butene (2). We have been investigating phases in Bi^{3+}/V^{5+}/A/O systems where A is Mg, Ca, Sr, and Ba. Known and structurally characterized quaternary phases in the Bi/Ca/V/O system are Bi$_2$CaV$_2$O$_9$ (3), BiCa$_9$V$_7$O$_{28}$ (4), BiCa$_4$V$_3$O$_{13}$ (5), BiCaVO$_5$ (6), and Bi$_6$Ca$_{18}$V$_{22}$O$_{82}$ (7). Among these phases, second harmonic generation was observed in BiCa$_9$V$_7$O$_{28}$, indicating possible potential as a nonlinear optical material (8). In this paper we report the synthesis and crystal structure of a new quaternary phase in this system, bismuth calcium vanadate, BiCa$_2$VO$_6$.

EXPERIMENTAL

A polycrystalline sample of BiCa$_2$VO$_6$ was synthesized using a stoichiometric mixture of Bi$_2$O$_3$ (Cerac, 99.999%), CaCO$_3$ (Mallinckrodt), and NH$_4$VO$_3$ (Johnson Matthey, 99%). The mixture was thoroughly ground, heated at 950°C for 30 hr, and then cooled to room temperature at a rate of 5°C/min. The pale yellow product was analyzed using an

electron microprobe, which confirmed a single-phase product with a Bi:Ca:V ratio of 1:2:1.

Powder X-ray diffraction data for BiCa$_2$VO$_6$ were collected using CuKα radiation on a Siemens D5000 diffractometer with vertical Soller slits and an energy-dispersive Kevex detector. Initial X-ray diffraction data were collected using a Si internal standard for the purpose of indexing and refinement of cell parameters. A second data set was then collected for Rietveld analysis without an internal standard. Details of data collection are given in Table 1.

Neutron diffraction data were collected on a 15-g sample of BiCa$_2$VO$_6$ at Brookhaven National Laboratory using the high-resolution powder diffractometer at beam line H1A of the high-flux beam reactor with a wavelength of 1.8857 Å. Further details of neutron diffraction data collection are given in Table 1.

Second harmonic generation was sought using a Nd^{3+}:YAG laser with a wavelength of 1064 nm.

STRUCTURE SOLUTION

Accurate peak positions for the first 30 reflections in the X-ray diffraction pattern were obtained using a pseudo-Voigt peak shape in the program Profile within the Siemens Diffract/AT suite (9). Diffractometer zero point and sample height errors were corrected using a Si internal standard. Autoindexing using the program Visser (10) suggested an orthorhombic cell with a figure of merit of $M_{20} = 227$. Cell dimensions were further refined using Refcel software (11), giving $a = 8.891(1)$ Å, $b = 11.950(2)$ Å, and $c = 5.542(1)$ Å. Systematic absences suggested two possible space groups: *Cmc*2$_1$ (No. 36) and *Cmcm* (No. 63) (12).

The second data set, collected without an internal standard, was used for application of direct methods and subsequent structure refinement. Initial attempts at structure solution were performed in space group *Cmc*2$_1$. Integrated intensities for the first 144 reflections were extracted using a Pearson profile function in the program Extra (13). Direct methods were applied to structure solution using the program Sirpow (14). This procedure suggested positions for Bi^{3+}, Ca^{2+}, and V^{5+}. Least squares refinement and subsequent difference Fourier synthesis within the GSAS suite

[1]To whom correspondence should be addressed.

TABLE 1
Details of X-Ray and Neutron Diffraction Data Collection
for $BiCa_2VO_6$

Quantity	X-ray diffraction data	Neutron diffraction data
a (Å)	8.89315(7)	8.8946(3)
b (Å)	11.9608(1)	11.9663(4)
c (Å)	5.54594(5)	5.5445(2)
Zero point (° 2θ)	− 0.0025(3)	0.0085(3)
Wavelength (λ)	1.54056	1.8857
Data range (° 2θ)	10–150	10–150
Step size (° 2θ)	0.02	0.05
Time per step (s)	10	300
Number of data points	6999	2802
Number of reflections	372	207
Number of variables	44	38
R_p (%)	7.41	9.39
wR_p (%)	10.22	12.10
R_F^2 (%)	4.43	12.11
χ^2	4.88	8.199

of programs (15) revealed four chemically plausible oxygen sites.

Subsequent Rietveld refinement of a total of 44 variables (scale factor, zero point, lattice parameters, 6 profile coefficients, 9 background terms, 17 positional parameters, and 7 isotropic temperature factors) gave an excellent agreement with the experimental diffraction pattern. Final agreement factors of $wR_p = 10.22\%$, $R_p = 7.41\%$, $R_F^2 = 4.43\%$, and $\chi^2 = 4.88$ were obtained.

Refined values of atomic fractional coordinates and isotropic temperature factors obtained from X-ray diffraction data were used as the starting model for refinement of neutron diffraction data. Upon refinement of a total of 38 variables (scale factor, zero point, lattice parameters, 5 profile coefficients, 9 background terms, 15 positional parameters, and 4 isotropic temperature factors), the obtained agreement factors were $R_p = 9.39\%$, $wR_p = 12.10\%$, $R_F^2 = 12.11\%$, and $\chi^2 = 8.199$. Observed, calculated, and difference curves for neutron diffraction data are shown in Fig. 1. The main obstacle to achieving an even better fit to the observed pattern was the inability to fully overcome the difficulties arising from highly asymmetric peak profiles inherent to data collected using neutron sources (14). This was confirmed by comparing the final agreement factors with those obtained by a LeBail fit to the observed pattern. Refinements were also attempted in space groups *Cmcm* and *C2cm*, and neither resulted in a satisfactory refinement.

Final refined parameters are given in Table 2, and selected bond distances and angles are given in Table 3. The relatively high standard deviations for vanadium parameters are due to the fact that vanadium is nearly invisible to neutrons.

STRUCTURE DESCRIPTION

The structure of $BiCa_2VO_6$ (Figs. 2 and 3a) can be viewed as consisting of covalently bound $(BiO_2)^-$ infinite chains and VO_4^{3-} tetrahedra with charge balance provided by interspersed Ca^{2+} cations. The cell dimensions of isostructural
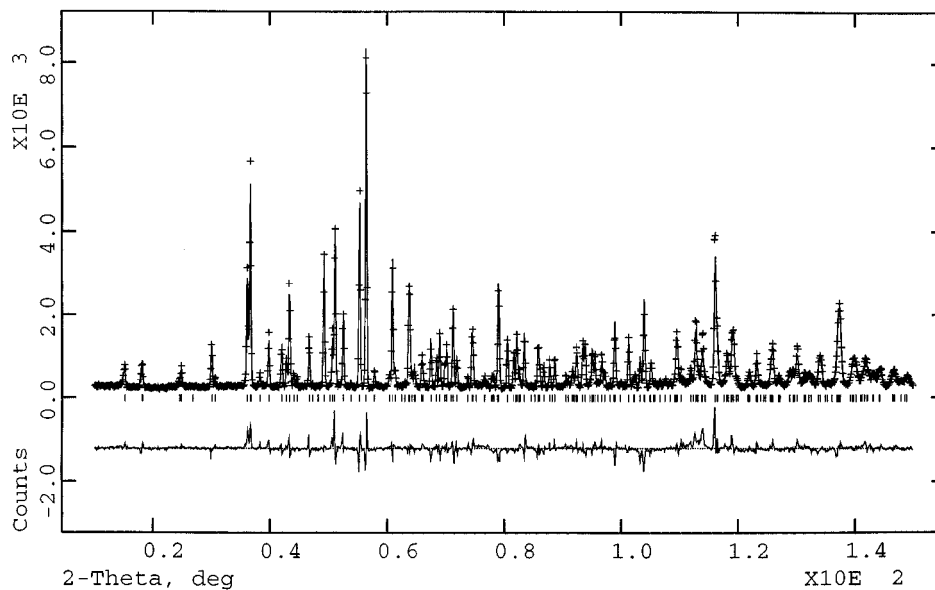

FIG. 1. Comparison of observed and calculated neutron diffraction powder patterns for $BiCa_2VO_6$ with difference pattern below.

TABLE 2
Atomic Fractional Coordinates[a] and Isotropic Thermal Parameters for BiCa$_2$VO$_6$

Atom	x/a	y/b	z/c	U_{iso} (Å)
Bi	0.5	0.0894(6)	0.25	0.00998(87)
	0.5	*0.09221*	*0.25*	
V	0	0.181(2)	0.199(4)	0.0126(9)
	0	*0.1979*	*0.25*	
Ca	0.2999(4)	0.3927(3)	0.242(1)	0.017(1)
Mg	*0.3084*	*0.4113*	*0.25*	
O(1)	0.3492(4)	0.9970(3)	0.492(1)	
	0.3319	*0*	*0.5*	0.0108(8)
O(2)	0	0.8168(3)	0.005(1)	0.00(1)
O(3)	0	0.9481(4)	0.568(1)	0.013(1)
O(4)	0.1548(4)	0.2472(3)	0.079(1)	0.0126(8)

[a] Values in italics are for BiMg$_2$VO$_6$.

TABLE 3
Selected Interatomic Distances (Å) and Bond Angles (°) for BiCa$_2$VO$_6$

	O(1)	O(2)	O(3)	O(4)
Bi	2.196(5) × 2	3.040(5)		3.008(5) × 2
	2.219(5) × 2			
V		1.696(23)	1.711(24)	1.720(15) × 2
Ca	2.285(7)	2.393(6)	2.780(6)	2.539(6)
	2.331(7)		2.622(7)	2.349(7)

O(1)–Bi–O(1) .... 77.83(9) × 2   O(2)–Bi–O(4) .... 71.1(2) × 2
O(1)–Bi–O(1) .... 75.4(2)   O(4)–Bi–O(4) .... 54.5(1)
O(1)–Bi–O(1) .... 74.5(2)

O(2)–V–O(3) .... 116(1)   O(3)–V–O(4) .... 104.5(9) × 2
O(2)–V–O(4) .... 112.4(9) × 2   O(4)–V–O(4) .... 106(1)

O(1)–Ca–O(1) .... 73.8(2)   O(1)–Ca–O(3) .... 80.7(2)
O(1)–Ca–O(2) .... 166.2(2)   O(1)–Ca–O(4) .... 90.5(3)
O(1)–Ca–O(3) .... 101.9(2)   O(1)–Ca–O(4) .... 108.6(2)

BiMg$_2$VO$_6$ (17), BiMg$_2$PO$_6$, and BiMg$_2$AsO$_6$ (18) are very similar to those of BiCa$_2$VO$_6$. Both structures (Figs. 3a and 3b) have the same (BiO$_2$)$^-$ infinite chains (Fig. 4) and VO$_4^{3-}$ tetrahedral units, but the orientation of the tetrahedra is very different in the two structures. A centric structure in space group *Cmcm* was found for BiMg$_2$*M*O$_6$ compounds

(17, 18). This structure and space group were used for Rietveld refinements of both the X-ray and neutron diffraction data for BiCa$_2$VO$_6$; no satisfactory result could be obtained. Further support for the acentricity of BiCa$_2$VO$_6$ was obtained by observation of a second harmonic generation
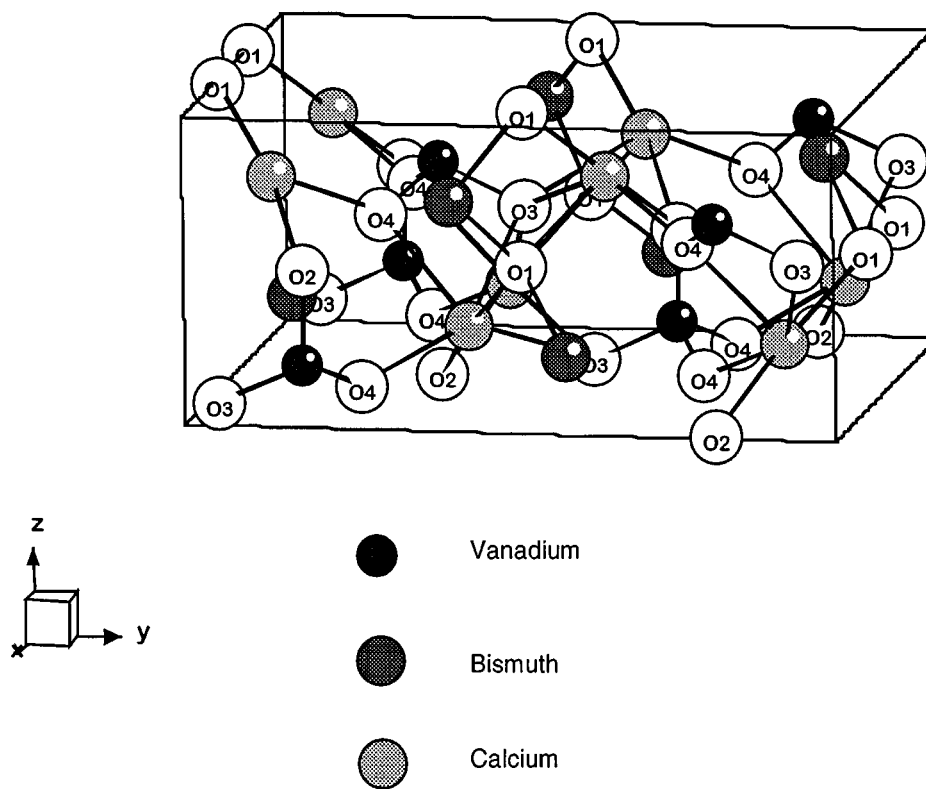

z
x → y

● Vanadium

● Bismuth

○ Calcium

FIG. 2. One unit cell of the structure of BiCa$_2$VO$_6$.
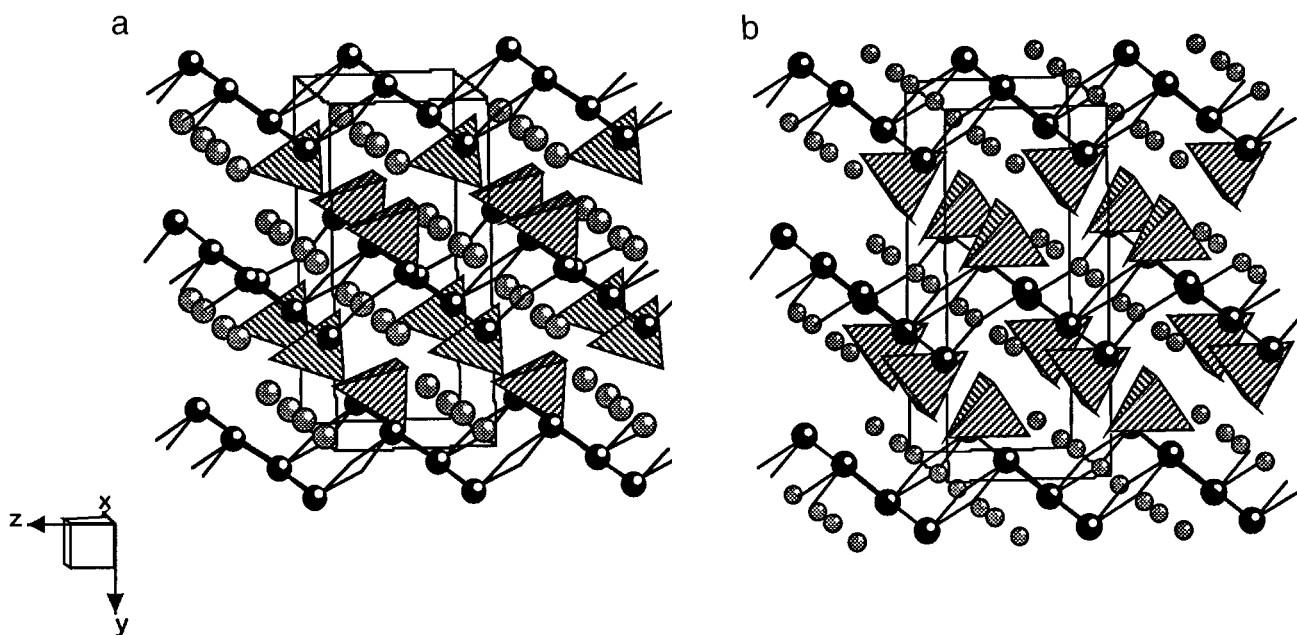
FIG. 3. Comparison of the structures of (a) $BiCa_2VO_6$ and (b) $BiMg_2VO_6$.

effect. An output intensity of about 1.5 times that of KDP was observed.

The coordination of Bi^{3+} in $BiCa_2VO_6$, $BiMg_2VO_6$, $BiMg_2PO_6$, and $BiMg_2AsO_6$ is typical of a lone-pair cation. On one side of Bi^{3+}, there are four short bonds of 2.2 Å. In the centric structure of $BiMg_2MO_6$ ($M = V, P, As$), the four short Bi–O bonds are constrained by space group symmetry to be equal. In acentric $BiCa_2VO_6$, the Bi^{3+} site is slightly distorted relative to that in the centric structure, now having two Bi–O distances at 2.196 Å and two at 2.219 Å (Fig. 4). The longer Bi–O bonds are to oxygen atoms of MO_4 tetrahedra. The orientation of these tetrahedra is very different in the centric and acentric structures. This then significantly impacts the nature of the long Bi–O bonds. In $BiCa_2VO_6$ there are three Bi–O distances of 3.0 Å (Fig. 5),

whereas in the $BiMg_2MO_6$ structure the shortest of the longer Bi–O distances is 3.5 Å.

The positions of V^{5+}, the A^{2+} cation, Bi^{3+}, and the oxygen of $(BiO_2)^-$ chains are compared in Table 2 for the $BiCa_2VO_6$ and $BiMg_2VO_6$ structures. The remaining oxygens are in very different positions due to the difference in the orientation of the tetrahedra. The A^{2+} cations are in essentially the same positions in the two structures, but, related to the different orientation of the tetrahedra, the coordination of Mg is fivefold whereas Ca is best described as coordinated to seven oxygens (Fig. 6). The larger size of Ca^{2+} relative to Mg^{2+} gives rise to the expected increases in the unit cell volume along with the a and c axes. However, the b axis in $BiCa_2VO_6$ (11.966 Å) is actually smaller than that of $BiMg_2VO_6$ (12.246 Å),
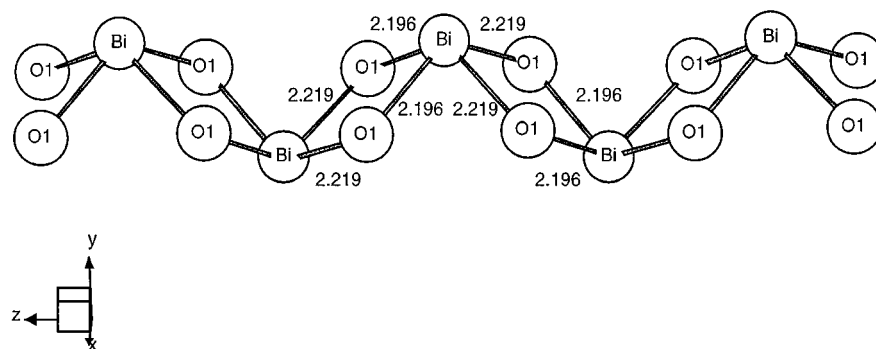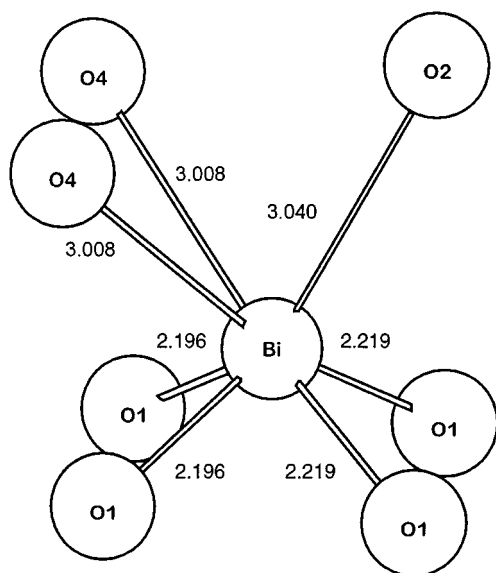

FIG. 4. $(BiO_2)^-$ chains in $BiCa_2VO_6$.

FIG. 5. Environment around Bi^{3+} in BiCa$_2$VO$_6$.

indicating better packing along the b axis in the BiCa$_2$VO$_6$ structure.

BiCa$_2$VO$_6$ can be considered a ferroelectric with the polar axis being the c axis. The distortion previously discussed in the (BiO$_2$)$^-$ chains can be considered a ferroelectric distortion. However, the biggest change in the BiCa$_2$VO$_6$ structure to switch polarity would be rotations
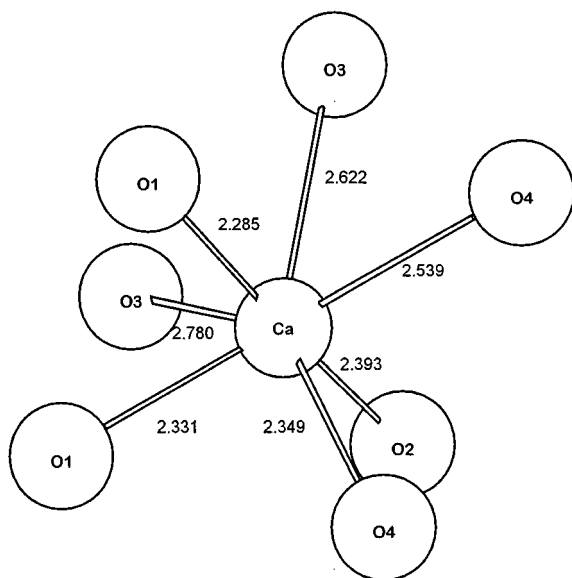
of VO$_4^{3-}$ tetrahedra. They all point in one direction along the polar axis. Switching the polarity of BiCa$_2$VO$_6$ would involve rotation of tetrahedra so that they all point in the opposite direction along the c axis. The centric BiMg$_2$MO$_6$ structure might be regarded then as the paraelectric form of BiCa$_2$VO$_6$. However, it is not obvious that the MO$_4$ orientation in the BiMg$_2$MO$_6$ structure would be on the lowest energy pathway for rotating VO$_4$ tetrahedra during ferroelectric switching in BiCa$_2$VO$_6$. At this time we have no evidence that BiCa$_2$VO$_6$ can be switched in an electric field, and we have no evidence of a transition to a paraelectric form below the melting point.

REFERENCES

1. J. D. Bierlein and A. W. Sleight, *Solid State Commun.* **16**, 69 (1975); A. W. Sleight, H.-y. Chen, A. Ferretti, and D. E. Cox, *Mater. Res. Bull.* **14**, 1571 (1979).
2. K. Aykan, D. Halvorson, A. W. Sleight, and D. B. Rogers, *J. Catal.* **35**, 401 (1974); A. W. Sleight, K. Aykan, and D. B. Rogers, *J. Solid State Chem.* **13**, 231 (1975).
3. J. S. O. Evans and A. W. Sleight, in preparation.
4. J. S. O. Evans, J. Huang, and A. W. Sleight, in preparation.
5. J. Huang and A. W. Sleight, *J. Solid State Chem.* **104**, 52 (1993).
6. J. Boje and Hk. Muller-Buschbaum, *Z. Anorg. Allg. Chem.* **619**, 521 (1993).
7. J. S. O. Evans and A. W. Sleight, in preparation.
8. A. W. Sleight and J. Huang, U.S. Patent 5202891, 1993.
9. A. Brown and J. W. Edmonds, *Avd. X-Ray Anal.* **23**, 361 (1980).
10. J. W. Visser, *J. Appl. Crystallogr.* **2**, 89 (1969).
11. J. K. Cockroft, Refcel software, V.3.03, 1995.
12. "International Tables for Crystallography" (T. Hahn, Ed.), Vol. 4. Kynoch Press, Birmingham, 1983.
13. A. Altomare, M. C. Burla, G. Cascarano, C. Giacovazzo, A. Guagliardi, A. G. G. Moliterni, and G. Polidori, *J. Appl. Crystallogr.* **28**, 842 (1995).
14. A. Altomare, G. Cascarno, C. Giacovazzo, A. Guagliardi, M. C. Burla, G. Polidori, and M. Camalli, *J. Appl. Crystallogr.* **27**, 435 (1994).
15. A. C. Larson and R. B. Von Dreele, "LANSCE," Los Alamos National Laboratory, Los Alamos, NM, 1994.
16. "The Rietveld Method" (R. A. Young, Ed.). Oxford University Press, Oxford, 1993.
17. J. Huang and A. W. Sleight, *J. Solid State Chem.* **100**, 170 (1992).
18. J. Huang, Q. Gu, and A. W. Sleight, *J. Solid State Chem.* **105**, 599 (1993).
19. R. D. Shannon, *Acta Crystallogr., Sect. A* **32**, 751 (1976).

FIG. 6. Environment around Ca^{2+} in BiCa$_2$VO$_6$.